

Platinum-group element sulpharsenides and Pd bismuthotellurides in the metamorphosed Ni-Cu deposit at Las Aguilas (Province of San Luis, Argentina)

FERNANDO GERVILLA

Instituto Andaluz de Ciencias de la Tierra and Departamento de Mineralogía y Petrología (Universidad de Granada-CSIC). Avda. Fuentenueva, s/n, 18002 Granada, Spain

ALEJANDRO SÁNCHEZ-ANGUITA

APLITEG S.L. Colonia de San Sebastián, 6-6ª, 18007 Granada, Spain

ROGELIO D. ACEVEDO

Centro Austral de Investigaciones Científicas, CONICET, 9410 Ushuaia, Tierra del Fuego, Argentina

PURIFICACIÓN FENOLL HACH-ALI

Instituto Andaluz de Ciencias de la Tierra and Departamento de Mineralogía y Petrología (Universidad de Granada-CSIC). Avda. Fuentenueva, s/n, 18002 Granada, Spain

AND

ANDRÉS PANIAGUA

Departamento de Geología, Universidad de Oviedo, Arias de Velasco s/n, 33005 Oviedo, Spain

Abstract

The Las Aguilas Ni-Cu-PGE deposit is associated with a sequence of basic-ultrabasic rocks made up of dunite, harzburgite, norite and amphibolite. These igneous (partially metamorphosed) rocks, and their host granulites, gneisses and migmatites of probable Precambrian age, are highly folded. The sulphide ore, consisting of pyrrhotite, pentlandite and chalcopyrite, occurs in the cores of both antiform and synform structures, within dunite, harzburgite and mainly along shear zones in bronzitite, replacing small mylonitic subgrains. The platinum-group mineral assemblage is dominated by Pd bismuthotellurides (Pt-free merenskyite, palladian bismuthian melonite and michenerite), with minor sperrylite, and PGE-sulpharsenides. The latter often occur as single, zoned crystals frequently showing cores of irarsite; outside these are concentric zones of cobaltian hollingworthite, rhodian nickelian cobaltite and Fe-rich nickelian cobaltite.

Mineralogical, textural and chemical evidence indicate that the sperrylite and platinum-group element sulpharsenides were formed during a primary magmatic event associated with the fractionation of a basaltic melt, which was contaminated by the assimilation of metamorphic crustal rocks. PGE sulpharsenides crystallized from As-bearing, residual magmatic liquids that collected PGE and segregated after the crystallization of the monosulfide solid solution. During high-grade metamorphism, sulpharsenides were remobilized as solid crystals in the liquated sulfides suffering partial dissolution and fracturing. On the other hand, there is no evidence of a primary concentration of Pd-bismuthotelluride minerals, and their present spatial distribution is only the consequence of their formation under high- to medium-grade metamorphism, down to temperatures of below 500°C. Pd bismuthotellurides crystallize even in fractures of sulpharsenides, attached to the boundaries of highly dissolved sulpharsenide crystals, and intergrown with molybdenite.

KEYWORDS: cobaltian hollingworthite, rhodian nickelian cobaltite, Pd bismuthotellurides, Ni-Cu ores, metamorphic reworking, Sierras Pampeanas, Argentina.

Mineralogical Magazine, December 1997, Vol. 61, pp. 861-877

© Copyright the Mineralogical Society

Introduction

THE Las Aguilas mining district is located 40 km to the northeast of San Luis city, in the San Luis Province of central Argentina (Fig. 1). It comprises two small bodies (Las Aguilas East and Las Aguilas West) of basic-ultrabasic rocks including dunite, harzburgite, bronzitite, norite, and amphibolite, hosted by high-grade metamorphic rocks (granulites, gneisses and migmatites). They belong to a set of occurrences of basic-ultrabasic rocks distributed in two narrow, NNE-SSW-oriented belts extending approximately 100 km northward from Las Aguilas. Metamorphic transformation of the magmatic rocks to amphibolite increases towards the north of the belts.

Exploration by the Dirección General de Fabricaciones Militares (DGFm) at Las Aguilas has shown the existence of a Fe-Ni-Cu sulphide mineralization mainly composed of pyrrhotite, pentlandite and chalcopyrite, and exclusively hosted by dunite, harzburgite and bronzitite (Sabalúa, 1986). This report also shows that bulk reserves exceed 2 million tons of ore with average grades of 0.51% Ni, 0.50% Cu and 0.035% Co, together with significant contents of platinum and palladium (up to 1.9 ppm

and 0.75 ppm respectively). Anomalously high Pt contents (17.8 ppm) have also been reported in one sample by Mogessie *et al.* (1995). To date, this, and the other mineralization associated with the northern basic-ultrabasic occurrences (Virorco, El Fierro, Manantiales...), are the only Ni-Cu-PGE deposits of interesting economic potential known in Argentina.

Previous papers on this deposit describe only local or preliminary petrographical and chemical data on both silicate and sulphide minerals (Malvicini and Brogioni, 1993; Gervilla *et al.*, 1993, 1994; Mogessie *et al.*, 1995), including some reports of platinum-group minerals (PGM). In this paper we describe the different species, spatial distribution and mode of occurrence of platinum-group, and other PGE-bearing minerals. Especial attention is paid to the genetic relationships between PGE sulpharsenides and Pd bismuthotellurides during their possible primary magmatic crystallization and subsequent metamorphic reworking.

Geology

The basic-ultrabasic bodies of the San Luis province crop out in the Sierras Pampeanas within the so-called Crystalline Basement which is also made up of

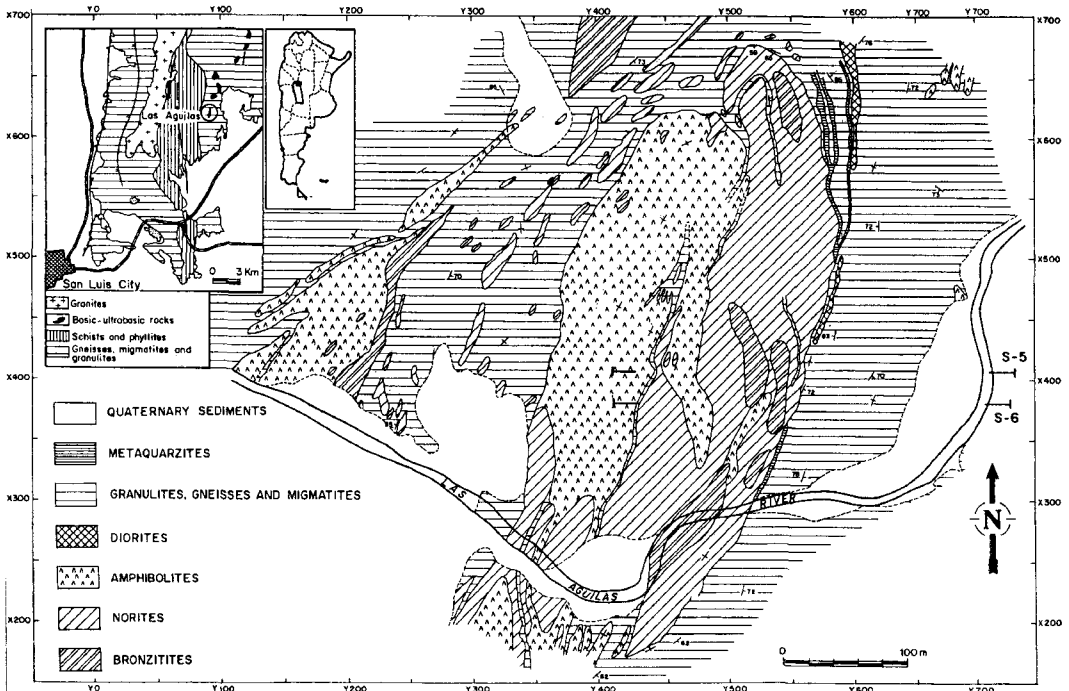


FIG. 1. Geological map of the Las Aguilas mine (modified from Sabalúa, 1986) indicating its geological and geographical location (upper left corner). S-5 and S-6 indicate the position of sections 5 and 6 of Fig. 2.

granites, pegmatites and, mainly, metamorphic rocks, including schists, phyllites, amphibolite, gneisses, migmatites and granulites. The age of these rocks is estimated as Late Precambrian to Ordovician.

According to Sabalúa (1986) the rocks of this region have suffered a complex, polyphased tectono-metamorphic evolution. Field relations and structural data indicate at least two events of deformation. The older event is characterized by vertical and asymmetric (vergent to the east) NNE–SSW-trending folds. This deformational event is responsible for the main foliation present in the region and its end is characterized by the development of shear zones parallel to the foliation resulting in abundant bands of mylonites. Data from Garcia-Casco *et al.* (pers. comm.) show that this event took place under granulite-facies conditions, at ≥ 7.5 kbar and $\geq 800^\circ\text{C}$, and mylonites developed during the retrograde, quasi-isobaric evolution. The younger deformation event generated similar but more open folds than the former, oriented in the direction N150°E. No foliation or metamorphism is associated with this event. During the Andean Orogeny the Crystalline Basement emerges as the consequence of NNE–SSW-, followed by E–W-trending normal faults giving rise to the formation of the Sierras Pampeanas range.

At Las Aguilas, the basic–ultrabasic rocks occur as two small bodies elongated in the direction NNE–SSW and dipping 80° – 85° to the east (Figs 1 and 2). Their shape is lenticular pseudo-tabular and they are highly folded, with ultramafic rocks in the cores of very asymmetrical, eastward-vergent anti-form (Las Aguilas-East) and synform (Las Aguilas-West) structures. From the cores to the limbs of such structures there are interlayered dunite and harzburgite, bronzitite, norite and amphibolite (Fig. 2). The country rocks are mainly sillimanite-bearing gneisses, and granulites near the contact with the basic–ultrabasic rocks. These metamorphic rocks can also be found as xenoliths within the igneous rocks. Both igneous and metamorphic rocks are locally cut by late dikes of diorite partly transformed into amphibolite.

The textural and mineralogical features suggest that the basic–ultrabasic rocks at Las Aguilas were originally formed by the crystal fractionation of a basaltic melt contaminated to a greater or lesser extent by the partial assimilation of xenoliths of metamorphic rocks. This suggestion is also supported by the chemical trends of the main silicate minerals (Gervilla *et al.*, 1993). These variations show significant Fe and Al enrichment in bronzite and, to a lesser degree in spinel, from dunite to bronzitite. Later, when plagioclase became a liquidus mineral, the availability of Al_2O_3 in the melt decreased, promoting Al impoverishment in both minerals and

the decrease in the modal proportions of spinel, giving rise to the formation of spinel-free norite. The disappearance of spinel from the mafic rocks is associated with the increase in the modal proportions of rutile. Iron enrichment in bronzite continues to norite and is positively correlated with the albite proportions of the coexisting plagioclase.

Although primary magmatic features can be recognized, they are frequently obliterated by later deformation and metamorphism. Major modifications are related to the recrystallization of previously deformed associations, the development of shear zones producing mylonitic bands and the amphibolitization of the igneous parageneses. The latter is very irregular but increases from the core to the limbs of the folds.

Sampling and analytical methods

The mineralogical data presented here relate to 52 samples selected from 45° -westward-dipping drill cores, 8 from Las Aguilas-East (4/1, 4/2, 5/2, 5/3, 5/4, 6/4, 6/5 and 7/4) and 3 from Las Aguilas-West (5W/1, 6W/1 and 7W/2), as well as samples collected along the Las Aguilas river, and from the dump of an exploration gallery in the Las Aguilas-East body. The precise location of the samples from the drill cores 5/2, 5/3, 5/4, 6/4 and 6/5 is shown in sections 5 and 6 in Fig. 2, selected as the most representative cross-sections of the Las Aguilas ore bodies.

The grains of precious metals were investigated in situ, in polished sections by reflected-light microscopy, systematic SEM scanning and EDS analyses, and by quantitative microprobe analyses. SEM microphotographs and EDS analyses were obtained using a Zeiss DSM 930 instrument equipped with a Link XQ 2000 microanalyser at the Centro de Instrumentación Científica of the University of Granada. Back-scattered electron images of grains were also acquired at the University of Granada using a CAMECA SX 50 electron microprobe operating at an accelerating voltage of 20 kV and a variable, but low beam current (3–10 μA). Electron-probe microanalyses were limited to the larger grains ($\geq 10 \mu\text{m}$), although the smaller ones were at least qualitatively characterized. They were obtained using a similar CAMECA SX-50 instrument at the Department of Geology of the University of Oviedo. The analyses were obtained using an accelerating voltage of 20 kV and a beam current of 20 μA . The X-ray lines measured were as follows: $K\alpha$ for S, Fe, Ni, Co and Cu; $L\alpha$ for As, Pd, Ir, Rh and Te, and $M\alpha$ for Pt and Bi. Corrections were made for the observed interferences between Pd and Rh, and Pt and Ir. The lower detection limit for the analysed elements is 0.1 wt.%. The standards used were synthetic PdTe_2 , PtTe_2 , Bi_2S_3 , and GaAs; natural

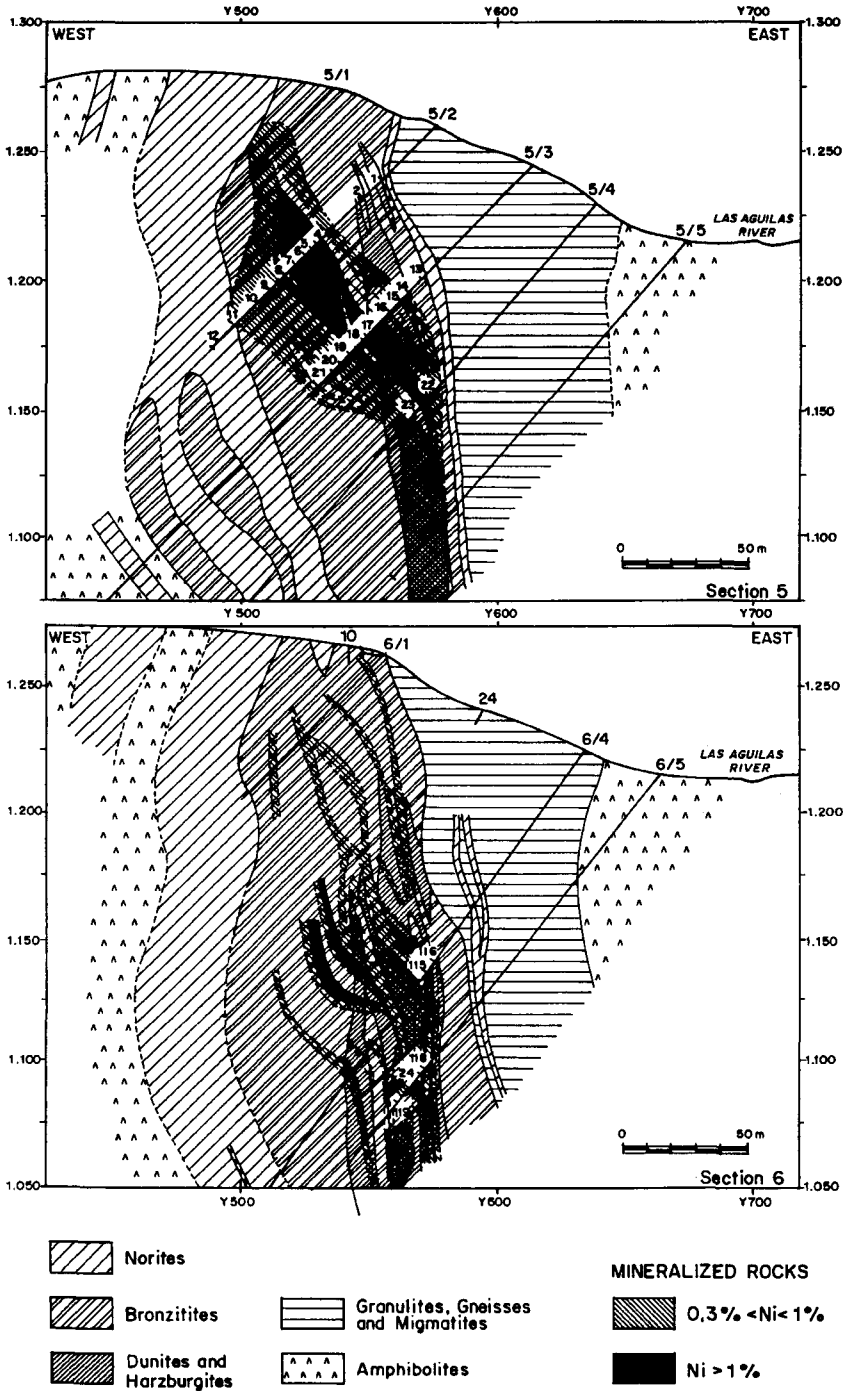


FIG. 2. Representative sections of the Las Aguilas-East body, indicating the position of drill holes 5/1 to 5/5, and 6/1 to 6/5, and the position of the samples collected from the drill cores (modified from Sabalúa, 1986). For simplicity, the samples are represented only by their numbers.

FeS₂ and CuFeS₂, and pure metals for Ni, Co, Ir and Rh. No standards of Os and Ru were available. Therefore, additional analyses of the sulpharsenides were kindly performed by Prof. G. Garuti at the University of Modena, using an ARL-SEMQ instrument, operating at 20 kV and 15 µA. The X-ray lines monitored were: K α for S, Fe, Ni and Co; L α for Ir, Ru, Rh, Pt, Pd and As, and M α for Os. The standards used were synthetic cobaltite, pyrite, nickeline and pure metals for PGE. No important Os and Ru contents were found, making both sets of analyses comparable.

Ore description

Textural relationships between sulphides and the host rocks vary from ultrabasic to basic rocks. Nevertheless the modal proportions of the main sulphide minerals (60% pyrrhotite, 25% pentlandite and 15% chalcopyrite) remain practically unchanged except near the borders of the xenoliths of

metamorphic rocks hosted by bronzitite, where a relative concentration of chalcopyrite takes place. Mineralized dunite typically exhibits a net texture with rounded to lobate olivine crystals (Fig. 3A). No primary inclusions of sulphides occur in olivine. When sulphides are scarce they tend to occupy vein-like, intergranular spaces, oriented parallel to the elongated olivine grains. Relatively frequent observations are made of minute grains of phlogopite, chlorite and carbonates associated with the sulphides. In harzburgite, sulphides tend to occupy a similar intergranular position. Intercumulus bronzite often contains primary inclusions of sulphides (Fig. 3B); however it usually occurs partly transformed into amphibole, showing sulphides as intergranular fillings of small cross-cutting veins and along the cleavage planes of the amphibole. More frequently than in dunite, sulphides occur associated (not in the primary inclusions) with carbonates, phlogopite, chlorite and locally apatite. In bronzitite, and in the rare mineralized norite, sulphides mainly follow the

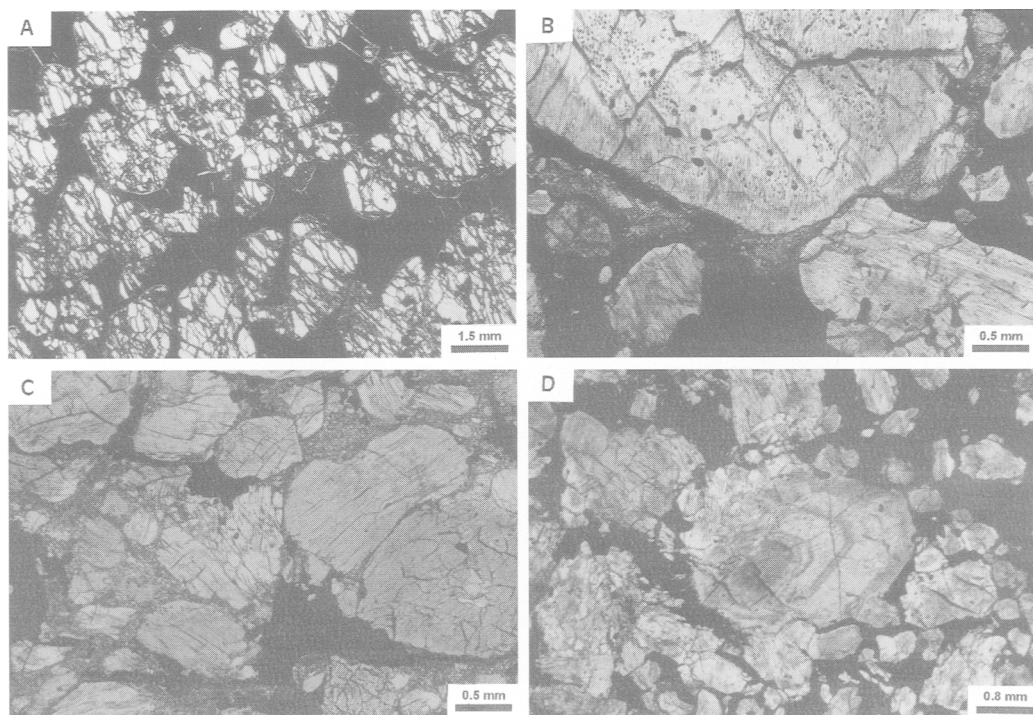


FIG. 3. Textural relationships between sulphides and silicate minerals under transmitted light and parallel nicols. A: Mineralized dunite. B: Mineralized bronzitite showing primary sulphide inclusions in a bronzite porphyroblast, and intergranular sulphides partially replacing the small mylonitic subgrains. C: Porphyroclastic texture (mortar texture) of a mineralized bronzitite showing the sulphides partially replacing the mylonitic subgrains. D: Mineralized bronzitite showing the primary zoning of a cumulus crystal of bronzite.

mylonitic bands replacing the small subgrains (Fig. 3B and C) tending to develop the characteristic texture of the mineralized bronzite, consisting of bronzite crystals with heterogeneous grain size and corroded borders, included in a sulphide matrix (Fig. 3D). In those bronzites located close to the contact with the ultramafic rocks, bronzite often shows primary rounded-to-idiomorphic inclusions of sulphides, mainly of pyrrhotite with flame exsolutions of pentlandite and rare chalcopyrite. Biotite and amphibole, and some chlorite, carbonates and apatite tend to occur at the contact between sulphides and major silicates, becoming more abundant (especially the biotite) towards the norite. Shear deformation also affects the xenoliths of metamorphic rocks included in the bronzite. In this case sulphides together with biotite, occur as intergranular replacements of the small subgrains of the mylonites and filling fractures in garnets. Disseminated sulphides also occur in the metamorphic country rocks, although their mineral association, mainly consisting of pyrite with minor pyrrhotite, is quite different from that of the basic-ultrabasic rocks.

The main sulphide assemblage in the mineralized basic-ultrabasic rocks consists of: (1) hexagonal pyrrhotite showing an annealed texture due to metamorphic recrystallization and locally transformed to monoclinic, with pentlandite exsolutions as oriented lamellae and 'flames'; (2) granular aggregates of pentlandite showing spot-like and along grain boundary alterations to violarite; and (3) intergranular chalcopyrite locally intergrown with cubanite, showing pseudo-eutectic myrmekitic intergrowths with pentlandite or partially transformed into bornite along fractures and at the contact with silicates. Chalcopyrite may also show lamellar inclusions of mackinawite. Primary pyrite is very scarce, although it is frequently found filling late veins. Accessory minerals (including PGE) are molybdenite, graphite, native gold, electrum, tell-

urobismuthite, altaite, PGE-bearing nickelian cobaltite, irarsite, cobaltian hollingworthite, sperrylite, michenerite, bismuthian merenskyite and palladian bismuthian melonite. Other late, secondary minerals are marcasite, goethite and covellite. Ilmenite and rutile are present in variable reciprocal proportions.

Electron microprobe analyses (Table 1) show that pyrrhotite contains 46 at.% metal (on average), relatively high Ni, varying from 0.30 to 2.87 wt.%, and low Co (<0.15 wt.%). Pentlandite shows significant Co contents, being higher in the bronzite-hosted ores (from 1.9 to 4.0 wt.%) than in dunite-hosted ores (from 1.2 to 1.8 wt.%). These data overlap the values reported by Malvicini and Brogioni (1993) in samples from the drill core 5/2. Chalcopyrite exhibits a stoichiometric composition with no detectable trace elements. On the contrary secondary pyrite occurring as vein fillings contains from 1.46 to 3.25 wt.% Co.

Platinum-group minerals

Arsenides and sulpharsenides

Sperrylite is the only arsenide found at Las Aguilas. It was first reported in one sample of drill core 5/3 by Mogessie *et al.* (1995) who describe crystals up to 200 µm in size with a stoichiometric composition. Nevertheless, after our detailed SEM and reflected microscopic investigations, only three minute grains (< 10 µm) of sperrylite included in pyrrhotite (2 grains) and in pentlandite (1 grain) have been detected, showing that although this mineral is present in the sulphide association, it is scarce and its occurrence is very random, thus explaining the local Pt anomalies in bulk-rock analyses (Sabalúa, 1986; Mogessie *et al.*, 1995).

In contrast to arsenides, sulpharsenides with a composition of nickelian cobaltite are ubiquitous minerals in the ore association at Las Aguilas. The

TABLE 1. Representative analyses of pyrrhotite (Po), pentlandite (Pn), chalcopyrite (Cp) and pyrite (Py)

		Weight percent							Atomic percent					
		S	As	Fe	Ni	Co	Cu	Total	S	As	Fe	Ni	Co	Cu
La-12-75	Po	40.74	n.d.	55.41	2.87	n.d.	n.d.	99.02	54.93	n.d.	42.90	2.11	n.d.	n.d.
La-12-76	Po	39.08	n.d.	59.07	0.78	n.d.	n.d.	98.93	53.17	n.d.	46.15	0.58	n.d.	n.d.
La-22-30	Po	39.86	0.16	59.15	0.33	n.d.	n.d.	99.50	53.81	0.09	45.84	0.24	n.d.	n.d.
La-22-26	Pn	33.43	n.d.	29.08	37.21	1.33	0.15	101.20	46.90	n.d.	23.43	28.52	1.02	0.11
La-11-69	Pn	33.57	n.d.	27.70	36.48	2.33	n.d.	100.08	47.50	n.d.	22.50	28.20	1.79	n.d.
La-19-22	Pn	32.96	n.d.	29.88	34.89	2.96	n.d.	100.69	46.56	n.d.	24.24	26.93	2.28	n.d.
La-10-85	Cp	34.89	n.d.	29.99	n.d.	n.d.	35.96	100.84	49.64	n.d.	24.50	n.d.	n.d.	25.82
La-110-B-15	Py	52.93	n.d.	44.35	n.d.	3.10	n.d.	100.38	66.10	n.d.	31.80	n.d.	2.11	n.d.

n.d.: not detected

grains studied exhibit an average grain size of approximately 50 μm . Their morphology varies from euhedral (Fig. 4A) to rounded, more or less fractured (Figs 5, 6 and 10), and although they occur within pyrrhotite or pentlandite, or intergranularly between both minerals, they tend to be located close to the contact between silicates and sulphides. Frequently, when they occur in mineralized shear zones far from the main sulphide ore body, they appear associated with hydrous minerals like amphibole, phlogopite and chlorite, showing corroded grain boundaries and/or extensive fracturing (Fig. 6). The studied nickelian cobaltite grains are isotropic or, rarely, very weakly anisotropic and exhibit a white colour with a variable bluish tint. This tint seems to be correlated with their PGE content.

One grain in the sample LA-19 shows extensive fracturing and abundant minute 'inclusions' of gold, electrum and merenskyite. Although at first glance

they might be regarded as true, primary inclusions, the fact that they always occur associated with, or within fractures (Fig. 5), shows that they postdate the fracturing of the pre-existing sulpharsenide, recording a late stage of PGE remobilization. On the contrary, primary rounded to idiomorphic inclusions of irarsite (Figs. 4 and 10) have been observed in at least 30% of the investigated crystals of nickelian cobaltite. Their size is very small, generally less than 3 μm , although relatively large grains ($\approx 10 \mu\text{m}$) have also been found (Fig. 4). The only irarsite crystal suitable to be analysed shows a sulphur-deficient composition ($\text{S}:\text{As} = 0.90\text{--}0.93$) with minor contents of Rh and Pd (Table 2). These kinds of irarsite inclusions in nickelian cobaltite is similar to those described by Häkli *et al.* (1976), Cabri (1981), Garuti and Rinaldi (1986) and Marchetto (1990), and as in the examples reported by Häkli *et al.* (1976) and Cabri (1981), they occur surrounded

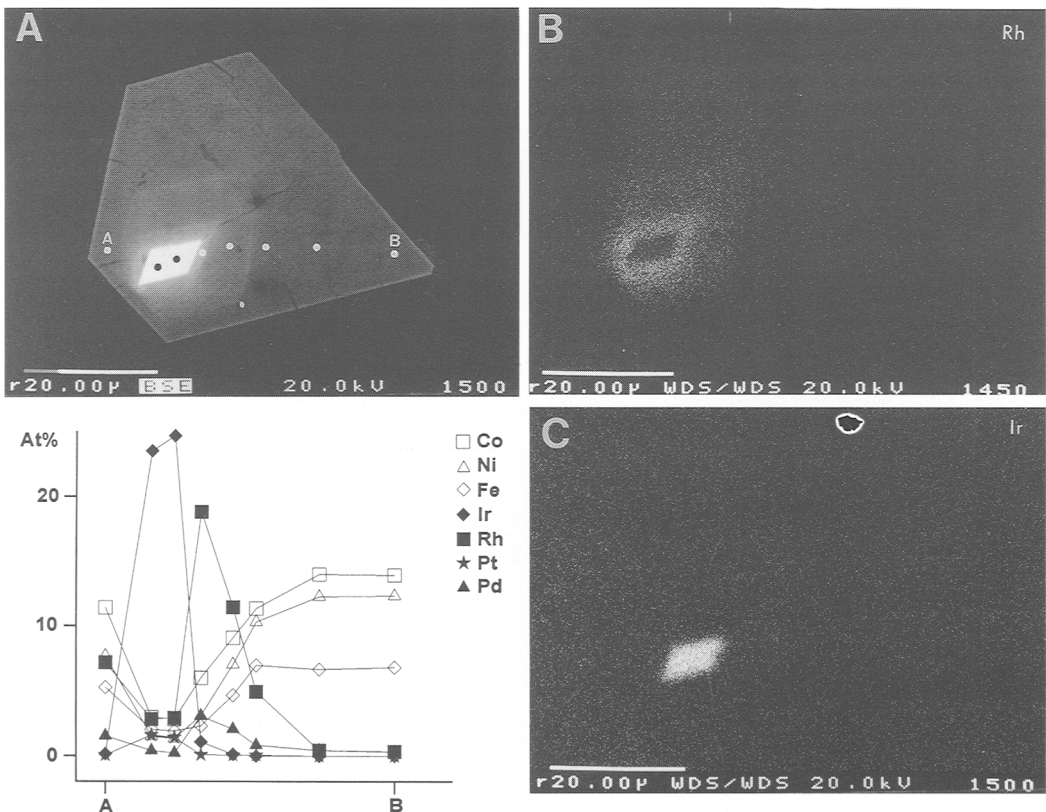


FIG. 4. Compositional zoning of a sulpharsenide crystal containing an irarsite inclusion. A: Back-scattered image of the crystal with the position of the analysed points. The microprobe results of the profile A–B are represented in the diagram below the photograph and are listed in Table 2 (analyses La-118-9 (point A) to La-118-2 (point B)).

B: X-ray image showing the distribution of Rh. C: X-ray image showing the distribution of Ir.

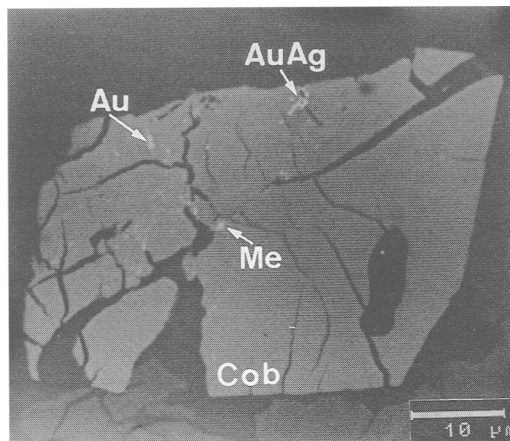


FIG. 5. Fractured crystal of nickelian cobaltite (Cob) showing minute grains of gold (Au), electrum (AuAg) and merenskyite (PdTe_2) along the fractures.

by concentric zones parallel to the crystal faces of irarsite (Fig. 4A) consisting of cobaltian hollingworthite, rhodian nickelian cobaltite and Fe-rich nickelian cobaltite with variable, but low, PGE contents (Table 2). An example of this kind of zoning is illustrated in Fig. 4, where three main zones can be distinguished on the basis of their PGE (mainly Rh) contents. The first one, attached to the irarsite grain boundaries, contains 29.38 wt.% Rh (18.82 at.%), 3.08 wt.% Ir (1.06 at.%) and 4.92 wt.% Pd (3.04 at.%). However, the narrowness of this zone (only 2.7 μm wide) along with the distribution

patterns of Ir and Rh shown in Fig. 4B and C, suggest that the above analytical results (in spite of the careful positioning of the beam) were slightly contaminated by both the adjacent irarsite and the second Rh-poorer zone. Hence Rh and Pd contents of this zone could be slightly higher (up to 31.11 wt.% Rh and 5.16 at.% Pd have been analysed in the irarsite-free, cobaltian hollingworthite grain of Fig. 6, Table 2). The second zone exhibits outwardly decreasing contents of these two PGE, from 19.25 wt.% Rh (11.41 at.%) and 3.56 wt.% Pd (2.04 at.%) to 8.88 wt.% Rh (4.92 at.%) and 1.53 wt.% Pd (0.82 at.%). This trend continues in the third zone where Rh decreases to 0.62 wt.% (0.33 at.%) and Pd to 0.54 wt.% (0.28 at.%). As shown in Fig. 6, similar zonings can also be observed in sulpharsenide crystals with no irarsite inclusions. These results together with those plotted in Fig. 7, provide evidence of an important capacity of Fe-rich nickelian cobaltite to dissolve Rh (and to a lesser extent Pd), suggesting a rather continuous solid solution series between hollingworthite and Fe-rich nickelian cobaltite end-members.

According to the experimental results in the system NiAsS-CoAsS-FeAsS (Klemm, 1965), the composition of the PGE-poor, Fe-rich nickelian cobaltite reported here corresponds to sulpharsenide crystals with a unit cell edge close to 5.62 Å that must have crystallized or re-equilibrated close to 600°C, and certainly above 550°C (Fig. 8). This can also be applied to most (Co,Ni,Fe) sulpharsenides reported in Cu-Ni sulphide deposits associated with basic-ultrabasic rocks (Cabri and Laflamme, 1976; Distler and Laputina, 1979; Cabri, 1981; Piispanen

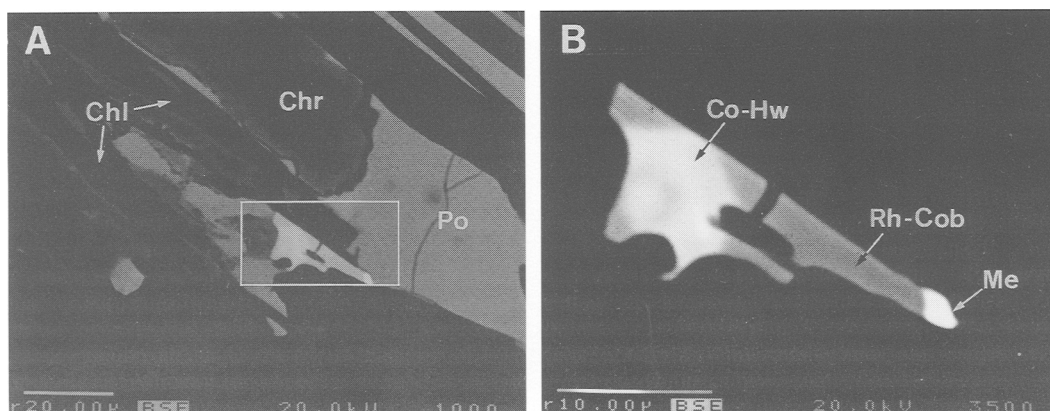


FIG. 6. A: Textural relationships of a highly dissolved sulpharsenide crystal with chlorite (Chl) pyrrhotite (Po) and partly oxidized chromite (Chr). B: Detailed back scattered image of the rectangular area marked in A, showing the zoning of the sulpharsenide, consisting of a cobaltian hollingworthite (Co-Hw) core surrounded by rhodian nickelian cobaltite (Rh-Cob). The image also shows the presence of a minute grain of Bi-rich merenskyite (Me) attached to the dissolved boundaries of the sulpharsenide.

TABLE 2. Representative analyses of sulpharsenides

Sample	Weight percent											Total
	S	As	Fe	Co	Ni	Os	Ir	Ru	Rh	Pt	Pd	
La-118-2	20.54	43.64	7.01	15.10	13.31	n.d.	n.d.	n.d.	0.62	n.d.	0.54	100.76
La-118-3	21.07	43.27	6.92	15.36	13.39	0.13	n.d.	0.10	0.80	n.d.	0.82	101.87
La-118-4	19.18	41.18	6.83	11.71	10.59	0.31	n.d.	0.22	8.88	0.17	1.53	100.60
La-118-5	17.29	39.80	4.27	8.77	6.76	0.46	0.34	0.32	19.25	0.15	3.56	100.95
La-118-6	15.54	37.71	1.92	5.35	2.72	1.11	3.08	0.32	29.38	0.25	4.92	102.30
La-118-7	10.60	27.45	1.13	1.76	0.82	0.10	51.04	n.d.	3.19	2.91	0.22	99.23
La-118-8	10.96	27.56	1.22	1.88	0.95	0.15	49.23	n.d.	3.13	3.33	0.46	98.86
La-118-9	17.85	40.77	4.87	11.12	7.45	0.94	0.45	0.21	12.23	0.14	2.64	98.66
La-118-1	20.33	42.59	7.12	13.63	13.97	n.d.	0.22	n.d.	1.24	n.d.	0.88	99.98
La-118-10	19.26	42.08	6.64	12.66	9.82	0.56	0.36	0.15	7.45	n.d.	1.47	100.45
La-120B-5	18.13	39.76	3.90	9.20	7.48	n.a.	0.12	n.a.	17.06	0.14	3.31	99.09
La-120B-5	17.58	37.79	2.72	6.87	4.55	n.a.	n.d.	n.a.	26.69	n.d.	4.51	100.71
La-120B-5	16.80	36.70	2.22	5.22	3.47	n.a.	0.34	n.a.	31.12	0.49	5.17	101.53
La-121	20.99	43.46	5.27	17.19	10.37	n.a.	n.d.	n.a.	0.46	n.d.	0.29	98.02
La-121	20.70	43.84	5.18	15.59	12.87	n.a.	n.d.	n.a.	0.41	n.d.	0.26	98.86

Sample	Atomic percent											Me/S+As
	S	As	Fe	Co	Ni	Os	Ir	Ru	Rh	Pt	Pd	
La-118-2	34.77	31.61	6.81	13.90	12.30	n.d.	n.d.	n.d.	0.33	n.d.	0.28	0.51
La-118-3	35.24	30.98	6.65	13.98	12.24	0.04	n.d.	0.05	0.42	n.d.	0.41	0.51
La-118-4	34.09	31.33	6.97	11.33	10.28	0.09	n.d.	0.12	4.92	0.05	0.82	0.53
La-118-5	32.89	32.41	4.66	9.08	7.03	0.15	0.11	0.19	11.41	0.05	2.04	0.53
La-118-6	31.94	33.17	2.27	5.98	3.06	0.38	1.06	0.21	18.82	0.08	3.04	0.54
La-118-7	30.75	34.08	1.88	2.78	1.30	0.05	24.70	n.d.	2.88	1.39	0.19	0.54
La-118-8	31.41	33.80	2.00	2.93	1.49	0.07	23.54	n.d.	2.79	1.57	0.39	0.53
La-118-9	33.59	32.83	5.26	11.38	7.66	0.30	0.14	0.12	7.17	0.04	1.49	0.51
La-118-1	34.83	31.22	7.00	12.70	13.07	n.d.	0.06	n.d.	0.66	n.d.	0.45	0.51
La-118-10	34.21	31.99	6.78	12.24	9.53	0.17	0.11	0.08	4.13	n.d.	0.78	0.51
La-120B-5	34.32	32.21	4.24	9.47	7.73	n.a.	0.04	n.a.	10.06	0.04	1.88	0.50
La-120B-5	34.33	31.59	3.05	7.30	4.85	n.a.	n.d.	n.a.	16.24	n.d.	2.65	0.52
La-120B-5	33.66	31.48	2.56	5.69	3.79	n.a.	0.11	n.a.	19.43	0.16	3.11	0.54
La-121	36.27	32.15	5.23	16.16	9.78	n.a.	n.d.	n.a.	0.25	n.d.	0.15	0.46
La-121	35.58	32.26	5.11	14.58	12.09	n.a.	n.d.	n.a.	0.22	n.d.	0.13	0.47

n.a.: not analysed

n.d. not detected

and Tarkian, 1984; Garuti and Rinaldi, 1986; Marchetto, 1990, among others), which also contain minor amounts of PGE (up to 7.2 wt.% Rh; Cabri, 1992). Considering that FeAsS molecular proportions in the Fe-poor regions of the system NiAsS–CoAsS–FeAsS, do not significantly affect the size of the unit cell (Klemm, 1965) or the structure, we can conclude (according also to Bayliss, 1969) that the structure of the PGE-poor nickelian cobaltite from Las Aguilas is cubic (Pa3) and rarely distorted, which explains the isotropic character of most of the studied grains. Ni substitution for Co further stabilizes the Pa3 structure

at the estimated temperatures. This means that high-temperature, Fe-rich nickelian cobaltite is isostructural with hollingworthite favouring the existence of the solid solution series suggested above.

Tellurides

Pd and Ni bismuthotellurides largely dominate the mineralogy of the platinum group elements in the Las Aguilas Ni-Cu deposit. They occur as rounded to subidiomorphic grains ranging in size between

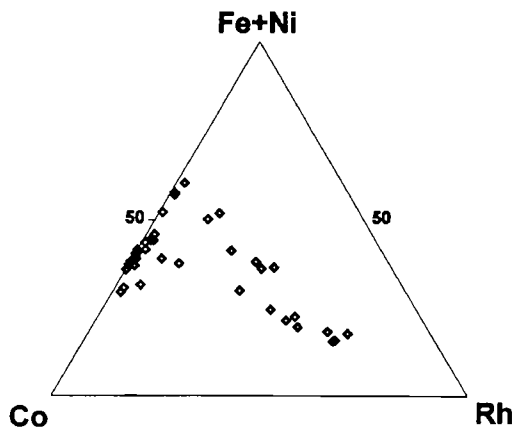


FIG. 7. Ternary plot showing the extent of the solid solution between nickelian cobaltite and hollinworthite in the studied samples.

1–2 μm and 100 μm (20 μm on average). Their textural relationship with the associated sulphide minerals is very variable (Fig. 9), occurring:

- (i) included in pyrrhotite (31 grains), in pentlandite (15 grains), or in chalcopyrite (20 grains);
- (ii) at the contact between pyrrhotite and pentlandite (10 grains), or between pyrrhotite and chalcopyrite (3 grains);
- (iii) at sulphide–silicate grain boundaries (23 grains); or
- (iv) attached to the grain boundaries of crystals of nickelian cobaltite (6 grains).

The latter occur locally associated with graphite (Fig. 9D) and two of the grains contain tiny inclusions of altaite which presents euhedral, hexagonal sections. In addition, 6% of all the studied grains occur associated, or intergrown with molybdenite (Fig. 10), and 11% of them have been observed within sulphide-filled fractures in garnets from a granulite xenolith present in bronzitite. As mentioned above, minute grains (<1 μm) of Pd tellurides, gold and electrum also occur along small fractures in a crystal of nickelian cobaltite (Fig. 5).

The most abundant telluride at Las Aguilas is merenskyite which presents an extensive substitution of Bi for Te and of Ni for Pd (Table 3, Fig. 11), varying in composition from $(\text{Pd}_{0.87}\text{Ni}_{0.14})_{\Sigma 1.01}(\text{Te}_{1.95}\text{Bi}_{0.04})_{\Sigma 1.99}$ to $(\text{Pd}_{0.94}\text{Ni}_{0.09})_{\Sigma 1.03}$

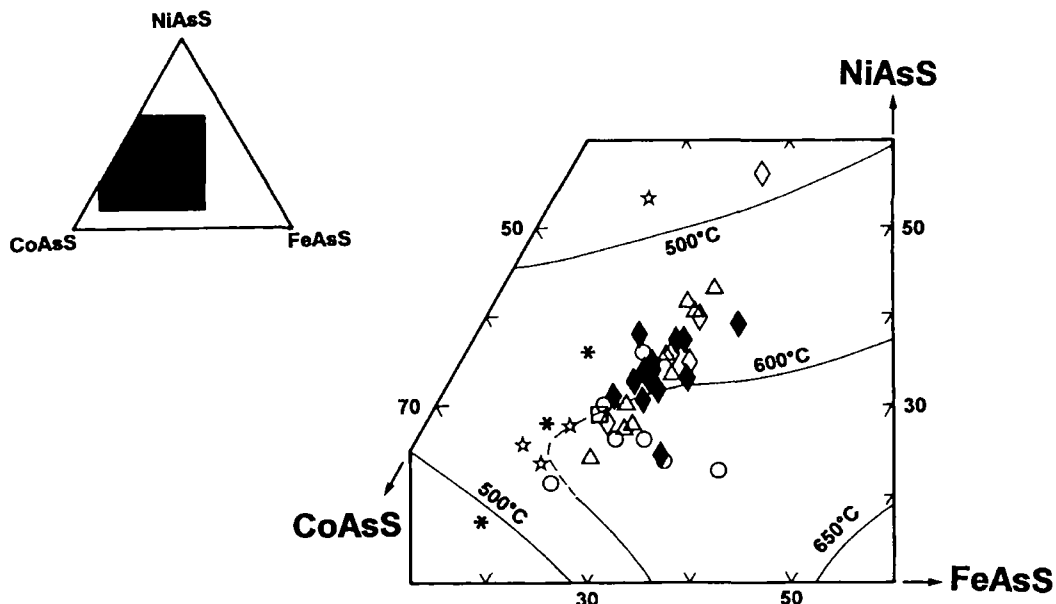


FIG. 8. Plot of the analysed nickelian cobaltite with less than 1 wt.% Rh (black diamonds), with reference to the solvus in the condensed system CoAsS–NiAsS–FeAsS at 500°C, 600°C and 650°C (Klemm, 1965). For comparison, we have also represented the composition of cobaltite-gersdorffite from other Ni–Cu deposits such as: Sudbury, Canada (Cabri and Laflamme, 1976; open diamonds), Pechenga, Russia (Distler and Laputina, 1979; stars), Pipe Mine, Canada (Cabri, 1981; squares); Rometölväs, Finland (Piispanen and Tarkian, 1984; asterisks); Ivrea Verbano, Italy (Garuti and Rinaldi, 1986; triangles) and O’Toole, Brasil (Marchetto, 1990, circles).

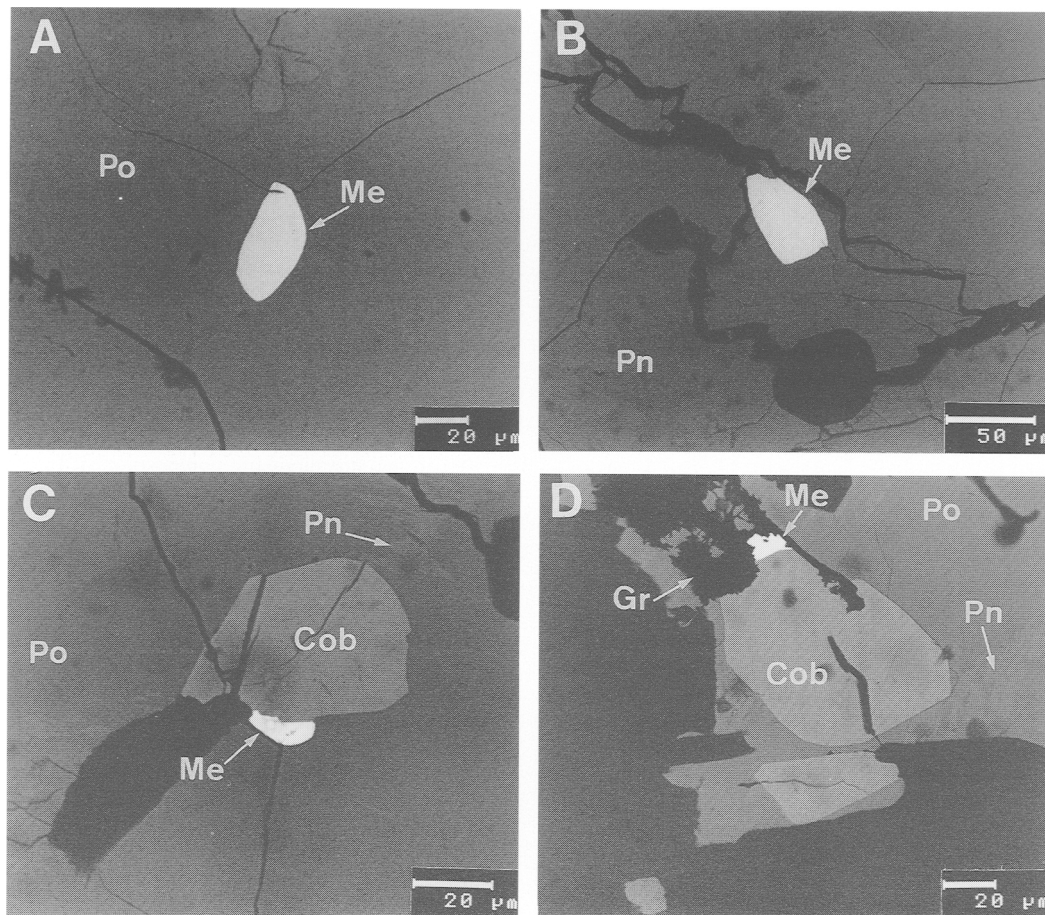


FIG. 9. Examples of occurrence of Merenskyite (Me). A: Included in Pyrrhotite (Po). B: Included in Pentlandite (Pn). C and D: Attached to the grain boundaries of cobaltite (Cob). Photographs C and D also show flame exsolutions of pentlandite (Pn) in pyrrhotite (Po) and D shows the association of merenskyite with graphite (Gr).

($\text{Te}_{1.39}\text{Bi}_{0.58}$) $\Sigma_{1.97}$ at the Pd-rich side of the diagram Pd/(Pd+Ni) vs. Bi/(Bi+Te) (Fig. 11B), and entering the palladian bismuthian melonite compositional field as far as ($\text{Ni}_{0.70}\text{Pd}_{0.33}$) $\Sigma_{1.03}$ ($\text{Te}_{1.81}\text{Bi}_{0.16}$) $\Sigma_{1.97}$. These compositional ranges show that the Ni- and Bi-free end-member of merenskyite has not been found and on the contrary that Bi substitution for Te approaches the maximum found experimentally by Hoffman and MacLean (1976), $\text{Pd}_{1.05}\text{Te}_{1.34}\text{Bi}_{0.61}$. The extent of Bi substitution for Te varies as a function of the Pd/(Pd+Ni) ratio of the merenskyite-melonite solid solution being higher for Pd-rich than for Ni-rich compositions. It is interesting to note that the grains analysed within sulphide-filled fractures in garnets are systematically Pd- and Bi-rich, and

overall merenskyite found at both sides of the central section of the orebody (section 5) presents progressively higher Bi/(Bi+Te) ratio (Table 3), showing a broad zoning in Pd-bismuthotelluride distribution. Platinum content is usually below the detection limits except in one large grain ($40 \times 80 \mu\text{m}$) included in pentlandite in a poorly mineralized dunite where it attained 7 wt.% Pt. The grain is not zoned and its average composition corresponds to the formula: ($\text{Pd}_{0.47}\text{Ni}_{0.40}\text{Pt}_{0.13}$) $\Sigma_{1.0}$ ($\text{Te}_{1.84}\text{Bi}_{0.15}$) $\Sigma_{1.99}$. Another unusual bismuthotelluride grain occurs in the sample LA-22 as one half of a biphasic inclusion in pyrrhotite. The other mineral in the inclusion is cubanite. Various electron microprobe analyses have shown that the composition of this grain varies from

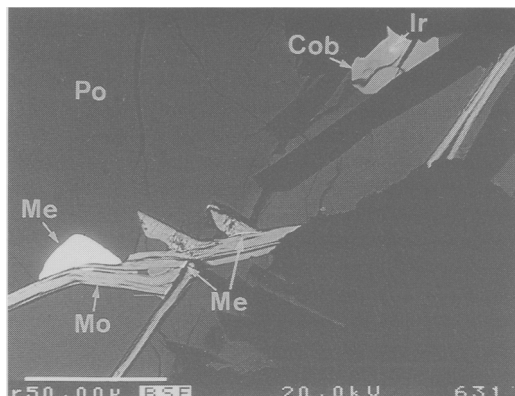


FIG. 10. Back scattered image showing merenskyite (Me) associated with, and intergrown with molybdenite (Mo). The picture also shows a dissolved and fractured crystal of nickelian cobaltite (Cob) with a rounded irarsite inclusion (Ir).

a palladian bismuthian melonite $[(\text{Ni}_{0.63}\text{Pd}_{0.33})_{\Sigma 0.96}(\text{Te}_{1.71}\text{Bi}_{0.32})_{\Sigma 2.03}]$ at the contact with the cubanite to a tellurobismuthite $[(\text{Bi}_{1.81}\text{Ni}_{0.1}\text{Pd}_{0.03})_{\Sigma 1.94}\text{Te}_{3.06}]$ at the opposite boundary (Gervilla *et al.*, 1994).

The optical and physical properties of merenskyite (colour, anisotropism and hardness) are relatively variable and correlate with the variability of its chemical composition. No significant changes have

been observed in relation to the Bi content of the merenskyite. On the contrary, the pure white colour (sometimes with a bluish tint in the studied samples) of this mineral becomes more creamy with an increasing Ni content, which also produces a change in the typical brown to greenish grey colours of anisotropy to yellowish brown-light grey, together with a slight decrease in hardness.

Only one grain of michenerite has been detected in the present study. It measures $28 \times 40 \mu\text{m}$ and occurs at the contact between pyrrhotite and pentlandite in massive sulphide ore, filling a 0.7 cm thick vein in bronzitite. Microprobe analyses (Table 3) show that the mineral represents a Pt-free, Ni-bearing composition corresponding to the formula $(\text{Pd}_{1.01}\text{Ni}_{0.03})_{\Sigma 1.04}\text{Bi}_{0.88}\text{Te}_{1.08}$. This mineral is slightly metal-enriched ($\text{Pd}+\text{Ni} = 34.59 \text{ at.}\%$) with respect to the stoichiometric composition of michenerite, contrary to the experimental results of Hoffman and MacLean (1976) who only found Pd-deficient compositions within a very narrow range (between 31.5 and 33.2 at.% Pd). Nevertheless, other metal-rich michenerites (especially platinumian michenerites) have also been reported in nature (e.g. Cabri and Laflamme, 1976; and Edgar *et al.*, 1989).

Mineral paragenesis

Although the genesis of the Ni-Cu-PGE ore at Las Aguilas cannot be unequivocally established, mainly due to the complexity of its metamorphic evolution, the mineralogical, textural and chemical features

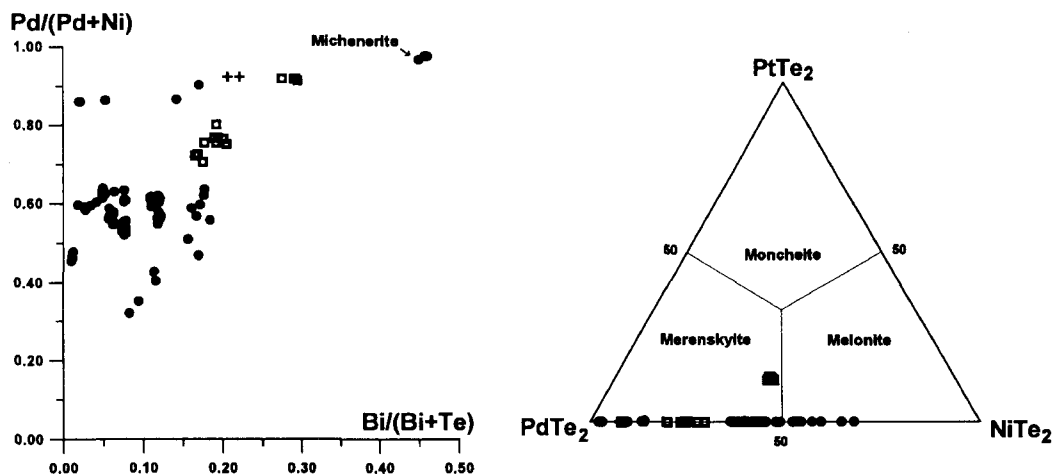


FIG. 11. Chemical composition of Pd-bismuthotelluride minerals in terms of their Pd/(Pd+Ni) and Bi/(Bi+Te) ratios (left), and their PtTe_2 - PtTe_2 - NiTe_2 molar proportions (right). Black circles: bronzitite-hosted ores; squares: dunitite-hosted ores; crosses: sulphide-filled veins in garnets from granulite xenoliths.

TABLE 3. Representative analyses of bismuthotellurides

Grain	n	Weight percent						Atomic percent				
		Te	Bi	Pt	Pd	Ni	Total	Te	Bi	Pt	Pd	Ni
La-7-4	5	68.84	5.95	n.d.	18.87	6.26	99.92	63.33	3.34	n.d.	20.81	12.52
La-11-1	5	67.64	7.01	n.d.	17.68	7.06	99.39	62.36	3.95	n.d.	19.54	14.15
La-16-1	13	64.72	8.52	6.82	13.89	6.51	100.46	61.53	4.95	4.24	15.83	13.46
La-18-1	3	67.06	8.40	n.d.	17.37	8.13	100.96	60.58	4.63	n.d.	18.82	15.97
La-19-4	6	66.87	7.83	n.d.	17.39	7.28	99.37	61.72	4.41	n.d.	19.25	14.61
La-110B-26	1	70.84	4.11	n.d.	18.24	6.83	100.02	64.36	2.28	n.d.	19.87	13.49
La-110B-35	1	66.55	6.12	n.d.	26.15	2.27	101.09	62.44	3.51	n.d.	29.42	4.63
La-112-1	4	71.85	3.26	n.d.	17.45	6.97	99.53	65.37	1.81	n.d.	19.04	13.79
La-112-3	5	74.45	1.34	n.d.	13.90	9.09	98.78	66.65	0.73	n.d.	14.92	17.69
La-114-1	5	45.48	30.38	n.d.	22.54	1.14	99.54	48.62	19.83	n.d.	28.89	2.65
La-114-3	7	54.79	20.95	n.d.	20.60	3.95	100.29	54.32	12.68	n.d.	24.49	8.51
La-115A-4	4	62.51	13.97	n.d.	17.06	6.16	99.70	59.60	8.13	n.d.	19.50	12.77
La-115A-7	8	62.66	13.68	n.d.	16.95	6.33	99.62	59.62	7.95	n.d.	19.34	13.09
La-116B-4	2	49.14	22.00	n.d.	26.80	1.22	99.16	50.47	13.80	n.d.	33.01	2.72
La-118B-B	3	32.35	43.07	n.d.	25.21	0.37	101.00	36.07	29.32	n.d.	33.71	0.90
La-118B-12	1	57.85	19.36	n.d.	13.42	8.33	98.96	55.68	11.38	n.d.	15.49	17.43
La-120A-5	1	57.20	20.19	n.d.	19.16	6.00	102.55	54.19	11.68	n.d.	21.77	12.36
La-120A-11	1	54.27	20.03	n.d.	17.52	7.64	99.46	52.11	11.74	n.d.	20.17	15.95
La-120B-3	2	63.77	13.56	n.d.	12.49	9.65	99.47	59.04	7.67	n.d.	13.87	19.43
La-120D-3	2	65.53	10.38	n.d.	10.95	11.88	98.74	59.13	5.72	n.d.	11.85	23.31
La-120D-4	2	57.99	18.34	n.d.	16.48	7.77	100.58	54.79	10.58	n.d.	18.67	15.96
La-121-1	2	70.47	2.44	n.d.	26.34	2.35	101.60	64.83	1.37	n.d.	29.06	4.70
La-123-4	1	58.59	15.96	n.d.	24.75	2.09	101.39	57.12	9.50	n.d.	28.93	4.43
La-124-3	2	55.42	18.68	n.d.	26.02	1.54	101.66	54.67	11.25	n.d.	30.78	3.30

n: number of analyses averaged from each grain

La-118B-B is the only grain of michenerite found

n.d.: not detected

described above strongly suggest that, at least two events played a very important role: a magmatic event, followed by extensive, syn- to post-metamorphic reworking.

The chemical and modal variations of the main silicate minerals of the host basic-ultrabasic rocks are consistent with their formation by crystal fractionation of a basaltic melt (Gervilla *et al.*, 1993), which could be contaminated by the assimilation of metapelitic rocks. This process gave rise to the observed sequence of dunite, harzburgite, bronzitite and norite. In addition, the presence of abundant, primary minute inclusions of sulphides in cumulus crystals of bronzite (never in olivine) shows that coeval with the crystallization of this mineral, the silicate melt became saturated in sulphur and segregated an immiscible sulphide melt. Although crystal fractionation by itself can saturate a basaltic melt in sulphur (e.g. Naldrett *et al.*, 1990), experimental studies reported in Buchanan and Nolan (1979) and Naldrett (1981) show that such a saturation can be more easily achieved by adding

both sulphur and silica to the system. At Las Aguilas, the assimilation of the surrounding, pyrite-bearing metapelitic rocks could supply the necessary sulphur and silica to make the fractionating basaltic melt enter the field of sulphide saturation. Thus, chalcophile elements partitioned to the immiscible sulphide melt, settling down to form the net texture characteristic of most mineralized dunite.

On the other hand, the close association between sulphide ore and shear zones (Fig. 3) clearly points to a late remobilization of the primary sulphides, which would originally be concentrated in the transition between dunite and bronzitite. This process was assisted by the presence or the intrusion of fluids, which probably favoured sulphide liquation. The latter is justified by the ubiquitous occurrence of amphibole, mica, chlorite, apatite and carbonates in the ore assemblage. Whether the fluids in question were metamorphogenic or were related to the magmatic intrusions responsible for the cross-cutting diorite dikes, remains unclear. However, the first hypothesis seems to be more realistic, taking

into account the NE–SW trending foliation observed in the amphibolitized dikes. As cited above (Sabalúa, 1986), the main foliation is related to the older deformational/metamorphic event, and shear deformation took place at its end, generating mylonitic bands that acted as porous channels for the mobilization of the sulphides. Metamorphism in greenschist facies conditions can be observed locally in the basic rocks from Las Aguilas; it could give rise to additional, small scale remobilization of the sulphides.

The current chemical and textural features shown by the Fe-Ni-Cu sulphides indicate that mobilization and metamorphic recrystallization developed on the primary magmatic assemblage as a whole, showing no significant modal variations, for example between mineralized, net textured dunite and sulphide-filled veins in norite or in the garnets from the xenoliths. This is also supported by the small variation range of the ratio Ni/Cu in the Las Aguilas-East orebody (Sabalúa, 1986). The absence of hexagonal pyrrhotite–pyrite transformations together with the mean atomic percent of metal of the pyrrhotite show that the temperature of the metamorphism should be above 600°C, at 1 bar (Arnold, 1962; Toulmin and Barton, 1964). This thermal minimum slightly increases with increasing pressure (Scott, 1973). Such a thermal minimum is also consistent with the equilibration temperature recorded by the described PGE-poor, Fe-rich nickelian cobaltite. These arguments suggest that the sulphide ore at Las Aguilas was remobilized under high-grade metamorphic conditions, which is consistent with the metamorphic *P–T* path shown by the surrounding metamorphic rocks (García-Casco *et al.*, pers. comm.). Pyrite-filled veins and marcasite-, goethite- and covellite-bearing assemblages only represent local markers of the later stages of the retrograde history of the sulphide ore.

Experimental results in PGE-, As- and S-containing systems (Skinner *et al.*, 1976; Makovicky *et al.*, 1990, 1991, 1992; and Fleet *et al.*, 1993) show that PGM of arsenide and sulpharsenide could crystallize directly from sulphide melts. According to Fleet *et al.* (1993), the small amounts of arsenic dissolved in the parental sulphide melt would partition into a late residual liquid generated after the crystallization of the monosulphide solid solution (mss). This liquid collected PGE (mainly Pt, Ir and Rh) and crystallized in the form of sperrylite and the zoned sulpharsenides described here. The rather uniform zoning of these sulpharsenide crystals, showing the same pattern in the different grains studied, in comparison with the complexly zoned ones generated under typical hydrothermal conditions (e.g. Ohnenstetter *et al.*, 1991), indicates that they crystallized from the above-mentioned As-bearing residual sulphide

liquid, with the zoning being the consequence either of the subsolidus reequilibrium on cooling or of the epitaxial growth of progressively PGE-poor phases around a PGE-rich, more refractory nucleus. In any case, PGE-rich sulpharsenides (irarsite or cobaltian hollingworthite) from the core of zoned crystals should crystallize/equilibrate at higher temperatures than those ($\approx 600^\circ\text{C}$) shown by the composition of the nickelian cobaltite from the rim. Marchetto (1990) reports sperrylite inclusions in nickelian cobaltite that would be generated by a similar process; in fact, the mineral paragenesis described by this author at the O'Toole deposit strongly resembles that of Las Aguilas. Nevertheless, the rounded and lobate shape, together with the fracturing of many of the studied crystals, suggests that primary sulpharsenides were remobilized as solid crystals within the liquated sulphides, suffering dissolution and local fracturing. This process might have started at the end of the early, high-grade metamorphism, coeval with the main remobilization of sulphides, but it finished during the late metamorphism in greenschist facies conditions. The latter is exemplified by the association shown in Fig. 6, where a highly corroded crystal, preserving only part of its primary zoning (cobaltian hollingworthite plus rhodian nickelian cobaltite) occur attached to chlorite and associated with corroded crystals of chromian spinel that show oxidized rims of ferritchromite.

The role played by the Pd bismuthotellurides must be analysed in the light of their phase relations in the system Pd–Te–Bi (Hoffman and MacLean, 1976). According to these experiments, michenerite decomposes slightly above 500°C and although merenskyite is stable up to 740°C, its thermal stability strongly decreases with the substitution of Te for Bi. The relatively low decomposition temperature of Pd-bismuthotelluride minerals allow them to be transported even under conditions of moderately low-grade metamorphism. In recent years, such a possibility has been convincingly shown by a number of authors (McCallum *et al.*, 1976; Rowell and Edgar, 1986; Edgar *et al.*, 1989; Mogessie *et al.*, 1991; Watkinson and Melling, 1992; Cook and Wood, 1994, among others). These results indicate that the current zoned distribution of Pd bismuthotellurides at Las Aguilas, taking into account their composition, would have been generated at relatively low temperatures during the retrograde evolution of the ore, and locally associated with the late, retrograde greenschist metamorphism. Some described textural relationships, like the presence of merenskyite grains included in fractures in nickelian cobaltite, attached to the grain boundaries of highly dissolved nickelian cobaltite, or associated, or intergrown with molybdenite, further support the

above hypothesis. Nevertheless an early concentration of Pd bismuthotellurides from magma-derived solutions, later remobilized during the retrograde metamorphic evolution of the ore, cannot be ruled out.

The close spatial relationship between the present sulphide ore at Las Aguilas and its primary location along the dunite–bronze transition zone show that the remobilization of both sulphides and PGE was restricted and did not lead to dispersion over great distances. Furthermore, the high proportion of Pd-bismuthotelluride grains that occur associated with the sulphide minerals (73%; with only 18% included in chalcopyrite) compared to what would be expected from a pure hydrothermal reworking and deposition of PGE (e.g. McCallum *et al.*, 1976; Edgar *et al.*, 1989; and Watkinson and Melling, 1992), suggests a minor role played by fluids in the remobilization process. This is also consistent with the fact that although mica, amphibole, chlorite, apatite or carbonates are ubiquitously present in the ore association, no extensive hydrothermal alteration can be observed in the host silicate rocks, and also with the restricted effect of the greenschists metamorphism. The latter could be responsible for mineral assemblages like that shown in Fig. 6, where the crystallization of merenskyite takes place after the complete dissolution of the nickelian cobaltite (and part of the rhodian nickelian cobaltite) rim of the primary crystal, in an oxidizing, Cl- and F-bearing chemical environment (preliminary analyses show that the associated chlorite contains 0.03–0.075 wt.% Cl and 0.03–0.3 wt.% F).

Conclusions

1. The Ni-Cu sulphide ore at Las Aguilas shows a platinum-group mineral assemblage mainly composed of arsenides, sulpharsenides and bismuthotellurides.

2. Arsenides and sulpharsenides contain Ir, Rh, Pt, Pd and, to a much lesser extent, Os and Ru. They occur in the form of sperrylite and, mainly, of composite, uniformly zoned crystals, made up, from core to rim, of cobaltian hollingworthite, rhodian nickelian cobaltite and nickelian cobaltite. Cobaltian hollingworthite often exhibits a core of Pt-poor irarsite. The chemical composition of these sulpharsenides provide evidence for an extensive solid solution between hollingworthite and Fe-rich nickelian cobaltite.

3. Pd bismuthotellurides are the most abundant PGM in the Las Aguilas Ni-Cu sulphide ore. Their composition mainly corresponds to Pt-free merenskyite with an extensive substitution of Bi for Te,

approaching the maximum found experimentally by Hoffman and MacLean (1976), and of Ni for Pd, entering the compositional field of palladian bismuthian melonite. Ni-bearing michenerite is very scarce.

4. A primary magmatic sulphide ore was formed by the segregation of an immiscible sulphide melt generated during the crystal fractionation of a basaltic melt contaminated by the assimilation of pyrite-bearing metamorphic rocks. The crystallization of the monosulfide solid solution gave rise to the segregation of an As-bearing residual liquid that collected PGE and crystallized in the form of sperrylite and the reported zoned sulpharsenides. No clear evidence of a primary concentration of Pd-bismuthotelluride minerals has been observed.

5. The sulphide ore was probably partly liquified, and remobilized along shear zones during, or slightly after, the main, high-grade metamorphism recorded in the region. Some remobilization continued later during greenschist metamorphism. The present zoned distribution of Pd-bismuthotelluride minerals, with progressively Bi-rich compositions away from the central portion of the deposit, is the consequence of such a continuous metamorphic reworking.

6. PGE sulpharsenides and Pd bismuthotellurides show a clear contrasting behaviour during the primary magmatic event and the subsequent reworking. The former crystallized originally from residual magmatic liquids and were remobilized as solid crystals in the liquated sulphide ore, suffering partial dissolution and fracturing. On the contrary, Pd bismuthotellurides were mainly associated with the metamorphic remobilization down to temperatures of below 500°C, crystallizing even in fractures of sulpharsenides and attached to the boundaries of highly corroded sulpharsenide crystals.

Acknowledgements

The authors are very grateful to the Dirección General de Fabricaciones Militares (Argentina) and specially to Colonel J.C. Delucchi and J.C. Sabalúa for the facilities given for the carrying on of this research, and for the permission to publish data from their internal reports. This work has been financially supported by the Junta de Andalucía (Research Group No 4028), the Dirección General de Investigación Científica y Técnica (Project AMB95-0512) and the Instituto de Cooperación Iberoamericana. We gratefully acknowledge the kindness of Prof. G. Garuti in performing certain problematic microprobe analyses and for our fruitful discussion during his stay in Granada. This paper is a

contribution to the I.G.C.P. Project No 336, *Intraplate Magmatism and Metallogeny*.

References

- Arnold, R.G. (1962) Equilibrium relations between pyrrhotite and pyrite from 325° to 743°C. *Econ. Geol.*, **57**, 72–90.
- Bayliss, P. (1969) X-ray data, optical anisotropism, and thermal stability of cobaltite, gersdorffite, and ullmanite. *Mineral. Mag.*, **37**, 26–33.
- Buchanan, D.L. and Nolan, J. (1979) Solubility of sulphur and sulphide immiscibility in synthetic tholeiitic melts and their relevance to Bushveld-Complex rocks. *Can. Mineral.*, **17**, 483–94.
- Cabri, L.J. (1981). The platinum-group minerals. In *Platinum-Group Elements: Mineralogy, Geology, Recovery* (L.J. Cabri, ed.) Can. Inst. Mining Metall. Spec., **23**, 83–150.
- Cabri, L.J. (1992) The distribution of trace precious metals in minerals and mineral products. *Mineral. Mag.*, **56**, 289–308.
- Cabri, L.J. and Laflamme, J.H.G. (1976) The mineralogy of the platinum-group elements from some copper-nickel deposits of the Sudbury area, Ontario. *Econ. Geol.*, **71**, 1159–95.
- Cook, N.J. and Wood, S.A. (1994) Platinum-group minerals in the Lac Sheen Cu-Ni-PGE prospect, Quebec. *Can. Mineral.*, **32**, 703–12.
- Distler, V.V. and Laputina, I.L. (1979) Nickel and cobalt sulpharsenides containing platinum metals. *Dokl. Acad. Nauk. SSSR, E.S.S.*, **24B**, 718–21.
- Edgar, A.D., Charbonneau, H.E. and McHardy, D.C. (1989) Pd-bismuthotelluride minerals at Rathbun Lake, Ontario: significance to post-magmatic evolution of PGE deposits. *Neues Jahrb. Mineral., Mh.*, **461**–75.
- Fleet, M.E., Chryssoulis, S.L., Stone, W.E. and Weisener, C.G. (1993) Partitioning of platinum-group elements and Au in the Fe-Ni-Cu-S system: experiments on the fractional crystallization of sulphide melt. *Contrib. Mineral. Petrol.*, **115**, 36–44.
- Garuti, G. and Rinaldi, R. (1986) Mineralogy of Melonite-group and other tellurides from the Iverano Basic Complex, Western Italian Alps. *Econ. Geol.*, **81**, 1213–7.
- Gervilla, F., Sabalúa, J.C., Carrillo, R., Fenoll Hach-Alí, P. and Acevedo, R.D. (1993) Mineralogy and mineral chemistry of the Las Aguilas Ni-Cu deposit (province of San Luis, Argentina). In *Current Research in Geology Applied to Ore Deposits* (P. Fenoll Hach-Alí, J. Torres-Ruiz and F. Gervilla, eds.), Servicio de Publicaciones de la Universidad de Granada, 461–4.
- Gervilla, F., Fenoll Hach-Alí, P., Acevedo, R.D., Carrillo, R. and Sabalúa, J.C. (1994) Minerales de Pd, Pt y Au del yacimiento de Ni-Cu de Las Aguilas (Provincia de San Luis). In *II Jornadas de Mineralogía, Petrografía y Metalogénesis de Rocas Ultrabásicas*. Publicación del Instituto de Recursos Minerales. Universidad Nacional de La Plata. **3**, 517–21.
- Häkli, T.A., Hänninen, E., Vourelainen, Y. and Papunen, H. (1976) Platinum-group minerals in the Hitura Nickel Deposit, Finland. *Econ. Geol.*, **71**, 1206–13.
- Hoffman, E. and MacLean, W.H. (1976) Phase relations of michenerite and merenskyite in the Pd-Bi-Te system. *Econ. Geol.*, **71**, 1461–8.
- Klemm, D.D. (1965) Synthesen und Analysen in den Dreieckdiagrammen FeAsS-CoAsS-NiAsS un FeS₂-CoS₂-NiS₂. *Neues Jahrb. Mineral., Abh.*, **103**, 205–55.
- McCallum, M.E., Loucks, R.R., Carlson, R.R., Cooley, E.F. and Doerge, T.A. (1976) Platinum metals associated with the hydrothermal copper ores of the New Rambler mine, Medicine Bow Mountains, Wyoming. *Econ. Geol.*, **71**, 1429–50.
- Makovicky, E., Karup-Møller, S., Makovicky, M. and Rose-Hansen, J. (1990) Experimental studies on the phase systems Fe-Ni-Pd-S and Fe-Pt-Pd-As-S applied to PGE deposits. *Mineral. and Petrol.*, **42**, 307–19.
- Makovicky, E., Rose-Hansen, J., Karup-Møller, S. and Makovicky, M. (1991) Factors governing concentration of platinum-group elements in layered complexes. *Final Report. European Economic Communities Contract No. MAIM-0006-DK.* (unpublished).
- Makovicky, M., Makovicky, E. and Rose-Hansen, J. (1992) The phase system Pt-Fe-As-S at 850°C and 470°C. *Neues Jahrb. Mineral., Mh.*, **441**–53.
- Malvicini, L. and Brogioni, N. (1993) Petrología y génesis del yacimiento de sulfuros de Ni, Cu y platinoideos "Las Aguilas Este", Provincia de San Luis. *Revista de la Asociación Geológica Argentina.*, **48** (1), 3–20.
- Marchetto, C.M.L. (1990) Platinum-group minerals in the O'Toole (Ni-Cu-Co) Deposit, Brazil. *Econ. Geol.*, **85**, 921–7.
- Mogessie, A., Stumpf, E.F. and Wiblen, P.W. (1991) The role of fluids in the formation of platinum-group minerals, Duluth Complex, Minnesota: mineralogic, textural and chemical evidences. *Econ. Geol.*, **86**, 1506–18.
- Mogessie, A., Hoinkes, G., Stumpf, E.F., Bjerg, E. and Kostadinoff, J. (1995) Occurrence of platinum group minerals in the Las Aguilas ultramafic unit within a granulite facies basement, San Luis Province, central Argentina. In *Mineral Deposit: from their Origin to their Environmental Impacts* (J. Pašava, B. Kříbek and K. Zák, eds), A.A. Balkema, Rotterdam. 897–900.

- Naldrett, A.J. (1981) Nickel sulphide deposits: classification, composition, and genesis. *Econ. Geol.*, 75th anniv. vol., 628–85.
- Naldrett, A.J., Brüggmann, G.E. and Wilson, A.H. (1990) Models for the concentration of PGE in layered intrusions. *Can. Mineral.*, **28**, 389–408.
- Ohnenstetter, D., Watkinson, D.H. and Dahl, R. (1991) Zoned hollingworthite from the Two Duck Lake intrusion, Coldwell complex, Ontario. *Amer. Mineral.*, **76**, 1694–700.
- Piispanen, R. and Tarkian, M. (1984) Cu-Ni-PGE mineralization at Rometölväs, Koillismaa Layered Igneous Complex, Finland. *Mineral. Deposita.*, **19**, 105–11.
- Rowell, W.F. and Edgar, A.D. (1986) Platinum-group element mineralization in a hydrothermal Cu-Ni sulphide occurrence, Rathbun Lake, northeastern Ontario. *Econ. Geol.*, **81**, 1272–7.
- Sabalúa, J.C. (1986) Yacimiento Las Aguilas. Mineralización Ni-Cu-Co, Departamento Pringles, Provincia de San Luis, República Argentina. Informe Final, *Dirección General de Fabricaciones Militares*, Mendoza. 32pp.
- Scott, S.D. (1973) Experimental calibration of the sphalerite geobarometer. *Econ. Geol.*, **68**, 466–74.
- Skinner, B.J., Luce, F.D., Dill, J.A., Ellis, D.E., Hagan, H.A., Lewis, D.M., Odell, D.A., Sverjensky, D.A. and Williams, N. (1976) Phase relations in ternary portions of the system Pt-Pd-Fe-As-S. *Econ. Geol.*, **71**, 1469–75.
- Toulmin, P. and Barton, P.B.Jr. (1964) A thermodynamic study of pyrite and pyrrhotite. *Geochim. Cosmochim. Acta*, **28**, 641–71.
- Watkinson, D.H. and Melling, D.R. (1992) Hydrothermal origin of platinum-group mineralization in low temperature copper sulphide-rich assemblages, Salt Chuck intrusion, Alaska. *Econ. Geol.*, **87**, 175–84.

[Manuscript received 25 March 1996:
revised 15 June 1997]